Hindawi

Research Article

Synthesis and Networking of Spaceborne Deployable Prismatic Antenna Mechanisms Based on Graph Theory

Jialong Zhu,[1,2] **Chuang Shi** (iD),[2] **Xiaodong Fan** (iD),[2] **Xiaofei Ma,**[1] **Hongwei Guo** (iD),[2] **Shikun Zheng,**[1,3] **and Rongqiang Liu**[2]

[1]*China Academy of Space Technology (Xi'an), Xi'an 710100, China*
[2]*State Key Laboratory of Robotics and System, Harbin Institute of Technology, Harbin 150001, China*
[3]*School of Mechano-Electronic Engineering, Xidian University, Xi'an 710071, China*

Correspondence should be addressed to Chuang Shi; ty12shichuang@126.com

Spaceborne deployable cylindrical antennas have broad application prospects in the fields of space earth observation and remote-sensing detection because of their significant advantages of ultralong aperture, high gain, and flexible beam scanning. As application requirements rapidly develop, a new type of spaceborne deployable cylindrical antenna mechanism with a large diameter and deployability is urgently needed. This paper presents an innovative design for a cylindrical deployable antenna mechanism based on 18R triangular prism elements based on graph theory. The correctness of the configuration is verified by developing a prototype. First, four kinds of nonoverconstrained 12-bar triangular prism-stabilized truss structure configurations and their corresponding topological diagrams are constructed. Second, based on graph theory, three types of 102 triangular prism-stabilized truss mechanism configurations that can be folded into linear mechanisms are derived. Third, the kinematic pair configuration is established to achieve a single-degree-of-freedom 7R2U9S triangular prism deployable unit. Fourth, combined with the geometric topology characteristics of the unit network, a triangular prism unit networking method is proposed, and a cylindrical network mechanism configuration based on 18R triangular prism units is obtained. A prototype was fabricated by 3D printing, and an expansion and retraction function test was conducted, which verified the correctness of the theoretical analysis in this paper. Finally, a new concept configuration for a parabolic cylindrical antenna is proposed. This paper provides a reference for the configuration of large-scale folding truss structures with unit expansion.

1. Introduction

The spaceborne deployable cylindrical antenna is an antenna form that can be folded into a small volume during the delivery stage and then deployed into a large-diameter cylindrical reflector antenna in orbit. It has broad application prospects in the fields of space earth observation and remote-sensing detection [1, 2]. Since its introduction in the Global Precipitation Mission (GPM) [3] in 2000, the realization form and related theoretical innovations for spaceborne deployable cylindrical antennas have emerged as a prominent area of research in the field of deployable antennas. As application requirements continue to evolve rapidly, further research should focus on meeting the demands for ultralarge apertures and scalable dimensions. In 2000, Eastwood et al. first

proposed a spaceborne deployable cylindrical antenna in the form of a deployable film antenna. The Kevlar film reflecting surface was driven by a chain-type deployable boundary mechanism to enable it to deploy and form. A prototype of a half-sized antenna measuring $2.6 \, m \times 2.6 \, m$ was used to develop the groundwork. Function and profile tests were carried out. However, the profile accuracy did not reach the expected index [4]. Alan and Sergio [5] introduced a scheme for a fixed surface deployment cylindrical antenna, which can be used to realize antenna deployment by driving four lightweight sandwich-curved panels through a self-locking hinge. Soykasap et al. [6] proposed the concept of a "hollow solid" structure, where the antenna is composed of carbon-fibre-reinforced plastic (CFRP) connected by flexible hinges. In the unfolded state of the antenna, this design

forms a thin-walled box structure with a high stiffness-to-mass ratio. Steven et al. [7] proposed a 108-long large-diameter cylindrical antenna composed of a supporting truss, a reflector, and a phased array feed. The overall structure of the antenna adopts a cable-rod modular structure, and the column is driven by a supporting truss, thereby enabling the overall deployment of the surface antenna. Based on the kinematic characteristics of the Bennett mechanism and the structural characteristics of the cylindrical antenna, Lv et al. [8, 9] and Song et al. [10] proposed two different forms of deployable cylindrical antenna networking mechanisms. The NEC Company in Japan [11] developed a spaceborne cylindrical reflector antenna product with a fixed surface and a deployable form. This system connects and drives three antenna cylindrical reflector panels through mechanical hinges to achieve expansion. In 2018, this company realized the first on-orbit application of a spaceborne cylindrical antenna. Dong et al. [12] proposed a method for constructing a frame-type deployable parabolic cylindrical antenna using a plane linkage mechanism. They also evaluated the design of the geometric configuration and completed the scale of the parabolic cylindrical antenna with a diameter of $30.12 \, \text{m} \times 100 \, \text{m}$. Lin et al. [13] developed a large-scale spaceborne deployable parabolic cylindrical antenna that adopted a modular frame-type deployable structure. This design enables the retraction and deployment of a cylindrical antenna with a diameter of $100 \, \text{m}^2$. Currently, the deployment of spaceborne cylindrical antennas is divided into four main categories, namely, film deployment, fixed surface deployment, shell-film deployment, and rod mechanism deployment. Among these methods, the rod mechanism deployable cylindrical antenna represents the prevailing approach for realizing super-aperture spaceborne cylindrical antennas measuring tens or even hundreds of metres across. The unit networking mechanism is characterized by modularity and deployability, which is suitable for the institutional form of superlarge deployable cylindrical antennas.

Configuration design serves as the cornerstone for mechanism research, enabling the synthesis of various types of mechanisms with needed motion forms. As the main realization form of the spatially deployable structure, configuration synthesis and design have been extensively investigated by many scholars. Herr and Horner [14] introduced a framed reflector design that uses a folding unit network to form a reflective surface. This configuration consists of a group of quadrilateral folding units networked in the same way as the reflector network and has a multiloop redundancy mechanism with good overall stiffness characteristics. Warnaar et al. [15, 16] used the method of graph theory to study the conceptual design of the deployable space mechanism, put forward a concept of a truss module based on graph theory, and studied the module as a basic unit to investigate the possibility of deploying the truss pattern. Andod [17] and Meguro et al. [18] introduced a hexagonal prism folding unit networking mechanism and realized the on-orbit splicing of ultralarge aperture antennas through modular networking units. Chen and Guan [19] proposed a hexagonal deployable unit driven by a telescopic rod, which served as the basis for designing a large-scale framed para-

bolic antenna. Vu et al. [20, 21] presented a method for constructing large-scale trusses using spatially deployable mechanisms. They analysed the relationship between large-scale trusses and the number of elements and element scale. They also defined structural efficiency indicators to evaluate the configuration and determine the optimal configuration. Zhao et al. [22] analysed the motion characteristics of deployable structures based on the scissor mechanism unit. They studied the process of using the scissor mechanism to form plane deployable structures, cylindrical deployable structures, and spherical deployable structures. Yang et al. investigated the configuration and kinematics of a quadrangular pyramid developable element based on a seven-bar closed-loop mechanism [23], a new hexahedral mechanism based on a spatial polyhedral centripetal mechanism [24], and a spatially symmetric 6R mechanism [25] and combined them. Different large-scale plane deployment mechanisms can be formed. Cui et al. [26] studied the kinematic characteristics of the Bricard linkage as a unit mechanism and proposed a configuration method for obtaining the antenna network deployment mechanism by splicing the Bricard linkage. Qi et al. [27] proposed two multielement combined configuration methods using the Myard linkage as a unit. They conducted kinematic analysis and parametric optimization for the new combined mechanism configuration. Xu et al. [28] introduced a deployable unit mechanism configuration method based on the helical theory to add constraint chains, and a new type of frame antenna triangular prism deployable unit mechanism configuration was obtained, which can be used to realize a uniform attitude for each node link during fully collapsed and deployed states. Shi et al. [29, 30] devised a series of conceptual configurations for double-layer ring truss antenna mechanisms based on the graph theory. They carried out mechanism design, analysis, and verification for one of the proposed configurations. Han et al. [31] conducted comprehensive research on the annular deployable antenna mechanism using the constraint synthesis method of the helix theory. The annular truss mechanism was divided into two parts: the upper and lower annular sides for analysis and synthesis. The current configuration for the unit networking mechanism is mainly realized using two different methods: One is to use the existing mature space exhibition mechanism as a folding unit and combine its movement characteristics to form a large-scale unit network mechanism by networking and splicing. This method demonstrates fast innovation speed and high maturity. This is the main way in which innovation is realized at this stage. However, as the demand for superlarge calibres increases, the use of large-scale existing mechanisms can lead to issues such as low overall stiffness, low storage ratio, and large weight. The second approach is based on the principles of mechanism configuration synthesis, combined with the demand motion form of the unit network mechanism to carry out the unit mechanism and network configuration synthesis.

Currently, a small number of methods, such as the helical theory constraint synthesis method and the mechanism graph theory method, are used to develop the parabolic deployable antenna mechanism. However, few results of innovative research on the configuration of a cylindrical

deployable antenna unit networking mechanism based on this method have been published. In the mechanism configuration method, the mechanism graph method is used to establish the topological relationship between the components and kinematic pairs through the topology diagram and its mathematical description. Subsequently, configuration analysis and synthesis are conducted based on the characteristics of the graph, which has a better effect on the unit network truss mechanism.

This paper focuses on addressing the requirements of unit networking in spaceborne cylindrical deployable antenna mechanisms. To this end, based on the method of graph theory, a new cylindrical deployable antenna mechanism based on 18R triangular prism elements is proposed. To achieve a larger aperture for the deployable antenna mechanism, a triangular prism unit networking method is proposed. Furthermore, a cylindrical network mechanism configuration is obtained based on 18R triangular prism units. A scaled-down prototype is developed to verify the deployment function and correctness of the theoretical analysis. The existing tensioning structures have multiple degrees of freedom, and the proposed deployable mechanism has a single degree of freedom. At the same time, this design combines the advantages of the high stiffness of the tensioning structure and the light weight of the cable net structure. Therefore, compared with the existing mechanisms, the proposed deployable mechanism has the advantages of easy driving, high stiffness, and light weight. In this way, one can realize large-scale deployable antenna mechanisms and provide new ideas for related engineering applications.

The sections of this paper are arranged as follows: In Section 1, according to Maxwell's geometric system stability criterion, a triangular prism element statically indeterminate truss structure that can be used for cylindrical antenna networking and its topology is constructed. In Section 2, the triangular prism unit truss mechanism configuration, the configuration topology description, and the kinematic pair configuration are completed. In Section 3, the unit networking geometric topology characteristics of the cylindrical antenna truss structure are combined. The principle prototype was produced by 3D printing, and an expansion and retraction function test was carried out to verify the correctness of the theoretical analysis in this paper. In Section 4, the concept for the configuration of a parabolic cylindrical antenna is designed.

2. Configuration Synthesis Based on Graph Theory

It is difficult to innovate and design many deployable mechanism configurations based on experience alone. Applying graph theory and other methods to the configuration synthesis of deployable mechanisms can help in the innovation of new deployable mechanisms, providing configuration references for the design of large modular spacecraft and prism mechanisms that can be stowed into straight lines.

A comprehensive truss structure configuration process is proposed based on graph theory (Figure 1). First, a unit-stabilized truss structure and its topology are constructed.

Second, according to the desired geometric constraints, the topological relationship for the variable links of the truss mechanism is synthesized by inserting the embryo diagram. Finally, according to the topology map and actual needs, the unit kinematic pair configuration is constructed, and the feasible mechanism configuration that meets the conditions is obtained. The detailed modelling process is shown in Reference [32].

2.1. Identification of Truss Structure Stability. According to Maxwell's criterion of necessary conditions for the stability of geometric systems, the following conditions must be satisfied for a stable truss structure:

$$e \geq \alpha v - \beta, \tag{1}$$

where e is the total number of sides; v is the total number of vertices; α is the dimension (the dimensions of the space, plane, and linear mechanisms are 3, 2, and 1, respectively); and β is the number of degrees of freedom, and the degrees of freedom of the space, plane, and linear mechanisms are 6, 3, and 1, respectively.

For the property of the truss structure map (undirected graph without self-closing transformation), we obtain the following:

$$\begin{cases} \sum_{i=\alpha}^{v-1} v_i = v, \\ \sum_{i=\alpha}^{v-1} i v_i = 2e, \end{cases} \tag{2}$$

where v_i is the number of points with degree i ($i = 1, 2, 3, \cdots$).

Equations (1) and (2) can be used to simultaneously solve for the feasible combination of vertex degrees and obtain the conceptual configuration of the demand-stabilized truss structure.

In addition, the adjacency matrix that corresponds to the map should be a symmetric square matrix M of order v and should satisfy the following properties:

(1) i satisfies $v - 1 \geq i \geq a (a = 1, 2, \text{ or } 3)$

(2) If the number of vertices is greater than $\alpha + 1$ and there are nonzero elements in both rows i and j, then $\alpha_{ij} = 0$

(3) At least one cycle satisfies $v = e$

(4) The number of vertices v and the number of edges e should satisfy Equation (2)

(5) All vertices are located in the outer circle

For the space triangular prism mechanism, $v = 6$, $\alpha = 3$, and $\beta = 6$. According to Equation (1), the total number of sides constituting a stable truss can be determined.
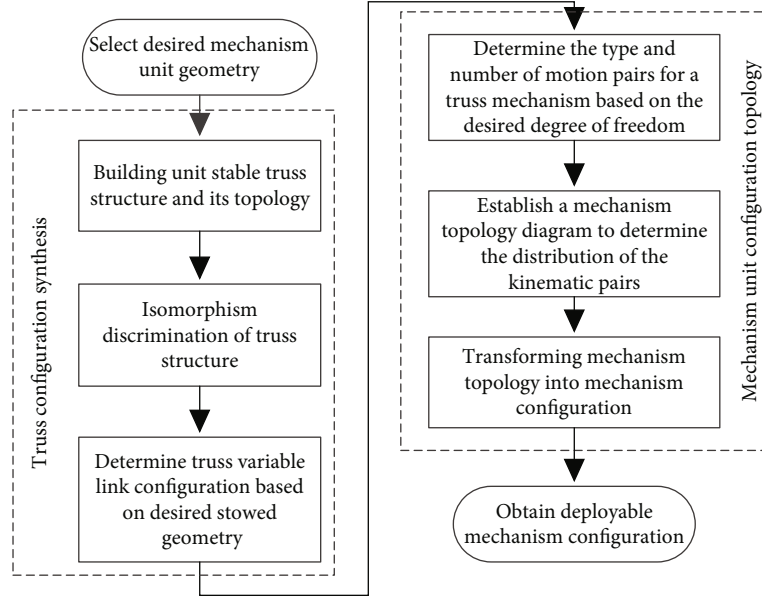
For the space triangular prism mechanism, we have $v = 6$, $\alpha = 3$, and $\beta = 6$. According to Equation (1), the total number of sides constituting a stable truss can be determined.

FIGURE 1: Comprehensive flow for the truss mechanism configuration based on graph theory.

$$e \geq 3 \times 6 - 6 = 12. \tag{3}$$

By setting the total number of edges to a minimum value of 12 and applying Equation (2), four possible configuration node combinations can be derived:

$$\begin{cases} C_1 = [v_3 = 0, v_4 = 6, v_5 = 0], \\ C_2 = [v_3 = 1, v_4 = 4, v_5 = 1], \\ C_3 = [v_3 = 2, v_4 = 2, v_5 = 2], \\ C_4 = [v_3 = 3, v_4 = 0, v_5 = 3]. \end{cases} \tag{4}$$

2.2. Establishment of the Topology Diagram for a Stable Truss. When considering the six vertices used to form a polygon on the outer ring for the triangular prism structure, we can set the corresponding element of the outer edge to 1. The corresponding adjacency matrix is obtained as shown in Figure 2.

To distinguish the different arrangement positions of the sides, a weighted adjacency matrix is introduced. The weight of the triangular sides (AB, BC, AC, DE, EF, and DF) at both ends of the triangular prism is 3. The weight of the two triangular edges (AF, BE, and CD) is 4. The weight of the newly introduced nonedge bars used to form a stable truss is 1. The weighted adjacency matrix is obtained as follows:

$$
\begin{array}{c|cccccc}
 & A & B & C & D & E & F \\
\hline
A & 0 & 3 & 3 & \_ & \_ & 4 \\
B & 3 & 0 & 3 & \_ & 4 & \_ \\
C & 3 & 3 & 0 & 4 & \_ & \_ \\
D & \_ & \_ & 4 & 0 & 3 & 3 \\
E & \_ & 4 & \_ & 3 & 0 & 3 \\
F & 4 & \_ & \_ & 3 & 3 & 0
\end{array} \tag{5}
$$

By adding 1 to the 6 vacancies of the upper triangular matrix, resulting in a total of 3 additions, and supplementing the lower triangular matrix based on symmetry, we can obtain the corresponding adjacency matrix with a total of 20 configurations. By counting the number of nodes with different degrees of truss knots for 20 configurations, two types of triangular prism trusses meet the combination $C_1 = [v_3 = 0, v_4 = 6, v_5 = 0]$, 12 types of triangular prism truss meet the combination $C_2 = [v_3 = 1, v_4 = 4, v_5 = 1]$, and 6 types meet the combination $C_3 = [v_3 = 2, v_4 = 2, v_5 = 2]$ for a triangular prism truss. However, no triangular prism truss type satisfies the combination $C_4 = [v_3 = 3, v_4 = 0, v_5 = 3]$.

2.3. Isomorphic Identification of Stable Trusses. The configurations obtained through different configuration synthesis methods can have different mathematical descriptions, but they are isomorphic. In this paper, the discrimination method based on the adjacency matrix correlation degree code [33] is used to discriminate isomorphism.

The graph correlation degree IDC is defined as follows:

$$\text{IDC} = \max \{\text{ID}_1, \text{ID}_2, \text{ID}_3, \cdots, \text{ID}_i, \cdots\}, \tag{6}$$

where $\text{ID}_i = d_{i1}, d_{i2}, d_{i3}, d_{i4}, \cdots, d_{ij}, \cdots, w_{i1}, w_{i2}, w_{i3}, w_{i4}, \cdots, w_{ij}, \cdots$; $d_{i1}, d_{i2}, d_{i3}, d_{i4}, \cdots, d_{ij}, \cdots$ denotes the degree of vertex j ($j = 1, 2, 3 \cdots$) adjacent to vertex i in the unit graph and $w_{i1}, w_{i2}, w_{i3}, w_{i4}, \cdots, w_{ij}, \cdots$ denotes the weight that connects vertices i and j.

A one-to-one correspondence was observed between the IDC code and unit map. If the IDC code is consistent, then an isomorphic configuration is obtained.

The isomorphism for the three combinations of six configurations that can be realized by the triangular prism structure was determined. Finally, three spatial triangular prism stable truss structure configurations were obtained, as shown in Table 1.
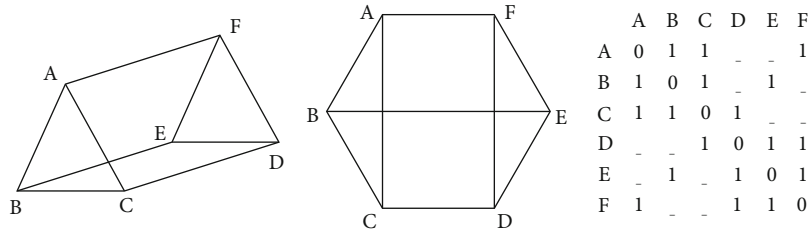
$$
\begin{array}{c|cccccc}
 & A & B & C & D & E & F \\
\hline
A & 0 & 1 & 1 & \_ & \_ & 1 \\
B & 1 & 0 & 1 & \_ & 1 & \_ \\
C & 1 & 1 & 0 & 1 & \_ & \_ \\
D & \_ & \_ & 1 & 0 & 1 & 1 \\
E & \_ & 1 & \_ & 1 & 0 & 1 \\
F & 1 & \_ & \_ & 1 & 1 & 0 \\
\end{array}
$$

FIGURE 2: Triangular prism structure and its topology.

TABLE 1: Summary of 12-bar 3-prism-stabilized truss types.

Serial number	Weighted adjacency matrix	Topology of trusses	Configuration sketch
Structure I	$\begin{array}{c\|cccccc} & A & B & C & D & E & F \\ \hline A & 0 & 3 & 3 & \underline{1} & \underline{0} & 4 \\ B & 3 & 0 & 3 & \underline{0} & 4 & \underline{1} \\ C & 3 & 3 & 0 & 4 & \underline{1} & \underline{0} \\ D & \underline{1} & \underline{0} & 4 & 0 & 3 & 3 \\ E & \underline{0} & 4 & \underline{1} & 3 & 0 & 3 \\ F & 4 & \underline{1} & \underline{0} & 3 & 3 & 0 \end{array}$		
Structure II	$\begin{array}{c\|cccccc} & A & B & C & D & E & F \\ \hline A & 0 & 3 & 3 & \underline{0} & \underline{1} & 4 \\ B & 3 & 0 & 3 & \underline{1} & 4 & \underline{0} \\ C & 3 & 3 & 0 & 4 & \underline{0} & \underline{1} \\ D & 0 & \underline{1} & 4 & 0 & 3 & 3 \\ E & \underline{1} & 4 & 0 & 3 & 0 & 3 \\ F & 4 & \underline{0} & \underline{1} & 3 & 3 & 0 \end{array}$		
Structure III	$\begin{array}{c\|cccccc} & A & B & C & D & E & F \\ \hline A & 0 & 3 & 3 & \underline{1} & \underline{1} & 4 \\ B & 3 & 0 & 3 & \underline{1} & 4 & \underline{0} \\ C & 3 & 3 & 0 & 4 & \underline{0} & \underline{0} \\ D & \underline{1} & \underline{1} & 4 & 0 & 3 & 3 \\ E & \underline{1} & 4 & \underline{0} & 3 & 0 & 3 \\ F & 4 & \underline{0} & \underline{0} & 3 & 3 & 0 \end{array}$		

2.4. Truss Structure Variable Rod Configuration. To construct a deployable truss mechanism from a stable truss structure, some of the rods must be modified into variable-length rods (folding rods or telescopic rods) to realize the mechanism employed to transition between folded and unfolded states. To fulfil the requirements of a high storage ratio during space transportation and ensure better adaptability to the space environment, the folded truss structure should maintain stability when the variable rods are fixed, and the truss mechanism should be optimized for linear

stability. Therefore, the number of fixed rods in the mechanism can be determined using Equation (1) subject to the following constraints:

$$
e_f \geq v - 1, \tag{7}
$$

where e_f is the total number of fixed rods.

For the folded truss structure composed of fixed rods, we obtain

TABLE 2: Statistics for the number of configurations of the triangular prism-stabilized truss type III that satisfy the parameters for the linear stabilized truss.

Serial number	Number of fixed-length rods	Variable-length rod quantity	Type of adjacency matrix that can be constructed	A nonisomorphic configuration conforming to the size constraint
1	5	7	792	79
2	6	6	924	21
3	7	5	792	2
4	8	4	495	0
5	9	3	220	0
6	10	2	66	0
7	11	1	12	0
8	12	0	1	0
Total number	—	—	3302	102

$$\begin{cases} \sum_{j=1}^{v-1} v_j = v, \\ \sum_{j=1}^{v-1} j v_j = 2e_f, \end{cases} \tag{8}$$

where v_j is the number of points with degree j ($j = 1, 2, 3, \cdots$).

Considering that the members of the truss mechanism are composed of variable and fixed rods, that is,

$$e = e_f + e_t, \tag{9}$$

where e_t is the total number of variable poles, including folding poles or telescopic poles.

By combining (11) and (13), the number of folding rods for the truss mechanism can be constrained as follows:

$$e_t \leq e - v + 1. \tag{10}$$

Taking the number of fixed rods that satisfy the constraints, the parallel vertical (11) and (12) can be used to obtain the node degree combination for the truss mechanism formed by the folded fixed rods and establish its topology map to obtain the corresponding truss mechanism.

Taking the triangular prism-stabilized truss type IV as an example, for a 12-bar triangular prism truss that can be folded into a linear mechanism, the number of fixed rods should exceed 5, and the number of folding rods should be less than 7, according to Equations (11) and (14). For the eight combinations of different fixed and variable rods, the configuration node type combinations of the linear mechanism under each combination can be solved using Equations (11) and (12), resulting in a total of 3302 types. Nondevelopable structures, including closed triangles, nondeployable closed quadrilaterals, and closed pentagons, are eliminated. After performing isomorphism discrimination, all 102 types of deployable linear truss structures for configuration III are obtained, as shown in Table 2. The deployable and stowed states are shown in Table 3. In Table 3, the rigid lines repre-

sent the fixed-length links, and the dashed lines represent the variable-length links. The four parameters in "Configuration x-x-x-x" represent the configuration number, number of fixed-length links, number of variable-length links, and configuration serial number, respectively. For example, "iii-7-5-1" represents configuration number III, 7 fixed-length links, 5 variable-length links, and a configuration serial number of 1.

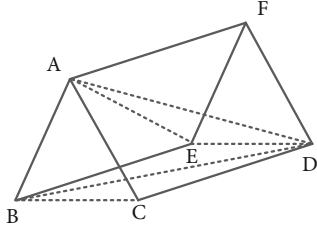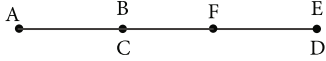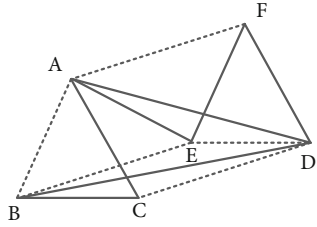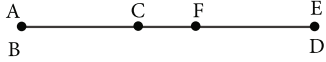Because the length of Table 3 is too long, the other parts of Table 3 are placed in Table 4.
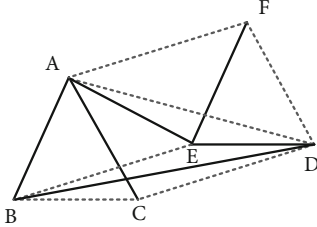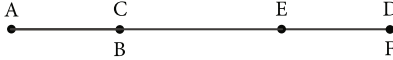
3. Kinematic Pair Configuration of the Triangular Prism Unit

The stable truss structure map provides a visualization of the geometric characteristics of the truss. However, to fully understand the composition and interconnections of the components, the diagram must be transformed into a topology map, which can then be used to determine the mechanism configuration kinematic pair configuration.

3.1. Matrix Description of the Institution Topology. According to the definition of mechanism topology, the mechanism topology diagram can be represented by an incidence matrix A and a c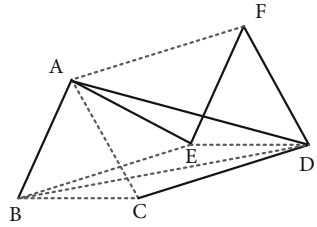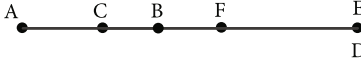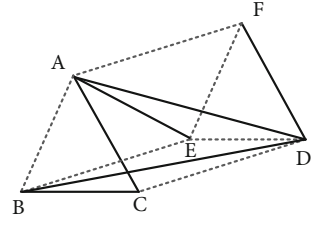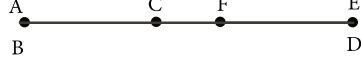omponent connection relationship adjacency matrix B. The associative adjacency matrix represents the connection between the vertices and links of all components of the configuration, and the component connection relationship adjacency matrix represents the correlation between components, the link, and the variable-length link and has a specific definition as follows:

(i) *The incidence matrix A for the mechanism*: a matrix that expresses the relationship between the vertices of the components and the components in the structure. $\alpha_{ij} = 1$ where vertex i belongs to component j, and $\alpha_{ij} = 0$ where vertex i does not belong to component j. It has the following characteristics: (1) Only two elements in each column are set to 1, and the rest are set to 0 because each edge is only associated

TABLE 3: Part of the type III 12-bar triangular prism truss mechanism configuration.

Serial number	Deployable truss configuration	Deployed	Stowed
1	Configuration III-7-5-1		
2	Configuration III-7-5-2		
3	Configuration III-6-6-1		
4	Configuration III-6-6-2		
5	Configuration III-6-6-3		

to two points. (2) A row of the incidence matrix is the association set of the corresponding vertex, and the number of nonzero elements in the row is equal to the degree of this vertex. (3) The complete incidence matrix can be used to describe the overall characteristics of the graph

(ii) *Component connection relationship adjacency matrix B of the mechanism*: used to represent the connection relationship between fixed-length rods and variable-length rods in the spatially deployable element. Definition: $\alpha_{ij} = 0$, which means that com-

ponents i and j are not connected; $\alpha_{ij} = 1$, which means that components i and j are connected at a single point; the elements on the diagonal line represent the connection between the component and itself; $\alpha_{ij} = 2$, which means that component i is connected to itself as a two-point connection, indicating that this link is a rod. Matrix A and matrix B have the following transformation relationship:

$$\mathbf{B} = \mathbf{A}^T \mathbf{A}. \qquad (11)$$

Table 4: Continuation of Table 3.

Serial number	Deployable truss configuration	Deployed	Stowed
6	Configuration III-6-6-4		
7	Configuration III-6-6-5		
8	Configuration III-6-6-6		
9	Configuration III-6-6-7		
10	Configuration III-6-6-8		
11	Configuration III-6-6-9		

Table 4: Continued.

Serial number	Deployable truss configuration	Deployed	Stowed
12	Configuration III-6-6-10		
13	Configuration III-6-6-11		
14	Configuration III-6-6-12		
15	Configuration III-6-6-13		
16	Configuration III-6-6-14		
17	Configuration III-6-6-15		

TABLE 4: Continued.

Serial number	Deployable truss configuration	Deployed	Stowed
18	Configuration III-6-6-16		
19	Configuration III-6-6-17		
20	Configuration III-6-6-18		
21	Configuration III-6-6-19		
22	Configuration III-6-6-20		
23	Configuration III-6-6-21		

TABLE 4: Continued.

Serial number	Deployable truss configuration	Deployed	Stowed
24	Configuration III-5-7-1		
25	Configuration III-5-7-2		
26	Configuration III-5-7-3		

TABLE 5: Incidence matrix for configuration III-7-5-1.

	AB	AC	AD	AE	AF	BC	BD	BE	CD	DE	DF	EF
A	1	1	1	1	1	0	0	0	0	0	0	0
B	1	0	0	0	0	1	1	1	0	0	0	0
C	0	1	0	0	0	1	0	0	1	0	0	0
D	0	0	1	0	0	0	1	0	1	1	1	0
E	0	0	0	1	0	0	0	1	0	1	0	1
F	0	0	0	0	1	0	0	0	0	0	1	1

TABLE 6: Adjacency matrix for the component connection relation for configuration III-7-5-1.

	AB	AC	AD	AE	AF	BC	BD	BE	CD	DE	DF	EF
AB	2	1	1	1	1	1	1	1	0	0	0	0
AC	1	2	1	1	1	1	0	0	1	0	0	0
AD	1	1	2	1	1	0	1	0	1	1	1	0
AE	1	1	1	2	1	0	0	1	0	1	0	1
AF	1	1	1	1	2	0	0	0	0	0	1	1
BC	1	1	0	0	0	2	1	1	1	0	0	0
BD	1	0	1	0	0	1	2	1	1	1	1	0
BE	1	0	0	1	0	1	1	2	0	1	0	1
CD	0	1	1	0	0	1	1	0	2	1	1	0
DE	0	0	1	1	0	0	1	1	1	2	1	1
DF	0	0	1	0	1	0	1	0	1	1	2	1
EF	0	0	0	1	1	0	0	1	0	1	1	2

The greater the number of fixed-length rods, the better the unfolded stiffness of the mechanism, which is more suitable for on-orbit applications. Therefore, taking the 12-bar unfolded truss type III-7-5-1 in Table 3 as an example for further configuration analysis, the incidence matrix and the adjacency matrix of the component connection relationship are shown in Tables 5 and 6, respectively.

3.2. Establishment of a Two-Colour Topology Map for the Mechanism.

According to the matrix description of the topology diagram, the complete topology diagram of the mechanism can be drawn, and the topology diagram shows the topology relationship between the components. To simplify the topological relationship between links, a two-colour topological diagram is used to describe it. The steps to create a two-colour topology map are as follows:

Step 1: fixed-length rods are represented by "•," and variable-length rods are represented by "o."

Step 2: the complete topological graph for each vertex obtained from the incidence matrix is called a partial complete graph. The partial complete graph at the vertex of the space-deployable unit can be simplified to a mechanism tree by removing some edges.

Step 3: when the local topology map is simplified into a tree, the priority as a local rack (all components are connected to this component) is fixed – length rod > collapsible rod, and the priority between the same type of rods is fixed according to their connection. The number of rods is sorted from most to least. If the number of fixed-length rods
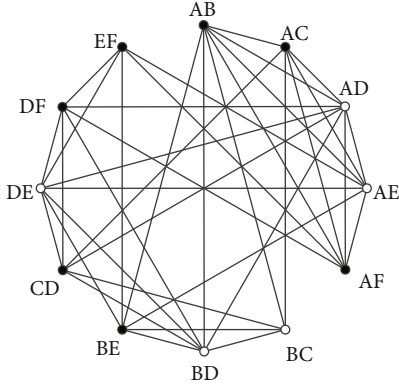
FIGURE 3: Two-colour complete topology for configuration III-7-5-1.

FIGURE 5: 7R2U9S motion pair configuration for triangular prismatic mechanism III-7-5-1.
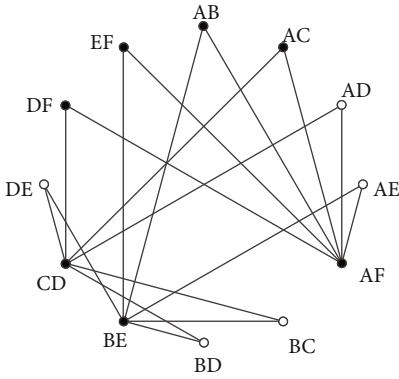

FIGURE 4: Two-colour map for configuration III-7-5-1.

connected by two rods of the same type is equal, the priority between them is sorted according to the number of foldable rods connected to them.

Step 4: the local rack and the whole rack must be consistent.

Step 5: if several qualified two-colour topology maps are obtained, then any one of them can be selected as the topology map that corresponds to the unit.

Taking configuration III-7-5-1 as an example, the complete two-colour topology can be obtained from the matrix (Table 6), as shown in Figure 3.

Merging the mechanism tree, the mechanism bicolour map for configuration III-7-5-1 can be obtained as shown in Figure 4.

Based on the two-colour topology diagram of the mechanism, according to the desired number of degrees of freedom of the mechanism, the number, type, and position of the kinematic pairs are configured. Considering the characteristics of space applications, the configuration should follow the following principles:

Rule 1: the hinge of the unit mechanism only adopts rotating, universal, and ball pairs.

Rule 2: ball pairs cannot be used at both ends of a link to avoid the introduction of local degrees of freedom.

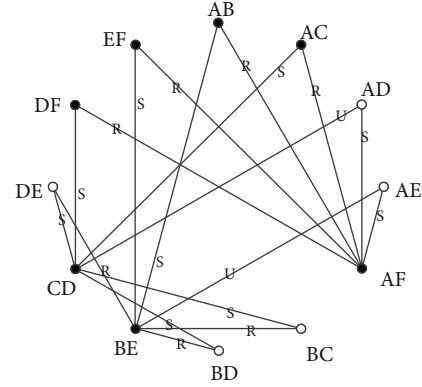*Rule 3*: each nonoverconstrained loop has at least 1 degree of freedom.

According to the equation for the degree of freedom of the space mechanism [33]:

$$M = 6(n - g - 1) + \sum_{i=1}^{g} f_i + \mu, \tag{12}$$

where M is the degrees of freedom, n is the total number of mechanism links (including racks), g is the total number of joints of the mechanism, f_i is the number of degrees of freedom of the i-th kinematic pair, and μ is the total number of allover constraints in the mechanism.

For the deployable truss and its two-colour topology map parameters, the variable-length rod can be regarded as a folding rod with an R pair (can also be regarded as a telescopic rod with a P pair) (R pair represents rotating pair and P pair represents moving pair), and then, Equation (12) can be expressed as follows:

$$M = 6((v + v_t) - (e_R + e_U + e_S + v_t) - 1) \\ + (e_R + 2e_U + 3e_S + v_t) + \mu, \tag{13}$$

where v is the total number of fixed and variable-length rods in the truss, v_t is the number of variable-length rods, e_R is the number of R pairs (rotating pairs), e_U is the number of U pairs (hook or universal hinges), and e_S is the number of S pairs (ball pairs).

Equation (13) can be simplified to obtain the following:

$$5e_R + 4e_U + 3e_S = 6v + v_t + \mu - M - 6. \tag{14}$$

For the two-colour topology, we have

$$e_G = e_R + e_U + e_S, \tag{15}$$

where e_G represents the total number of edges in a two-colour topology graph.
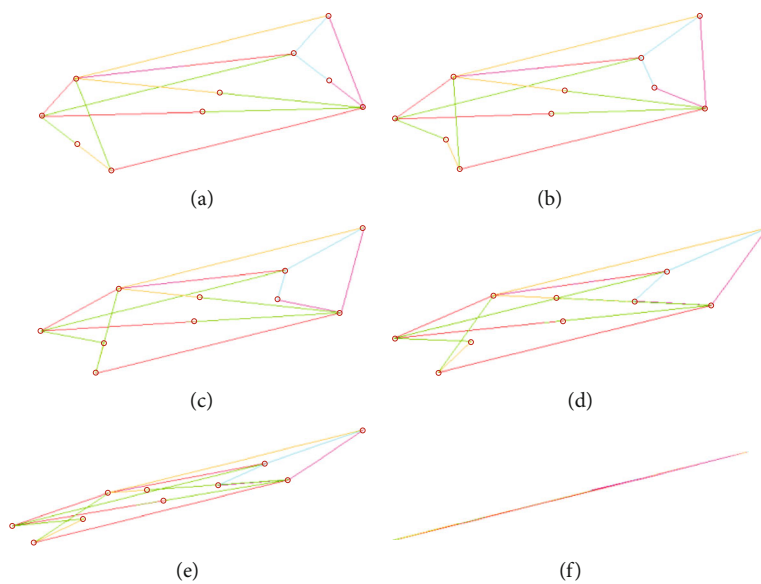
(a)   (b)

(c)   (d)

(e)   (f)

FIGURE 6: Triangular prism unit-deploying process.
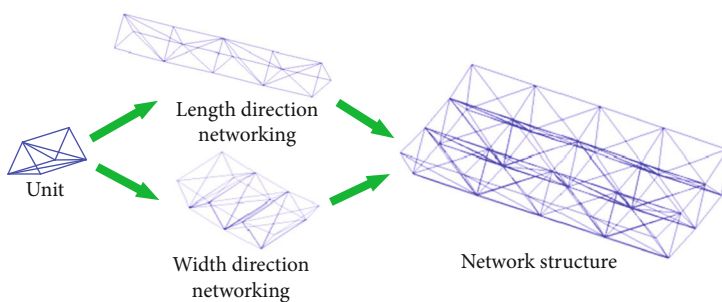

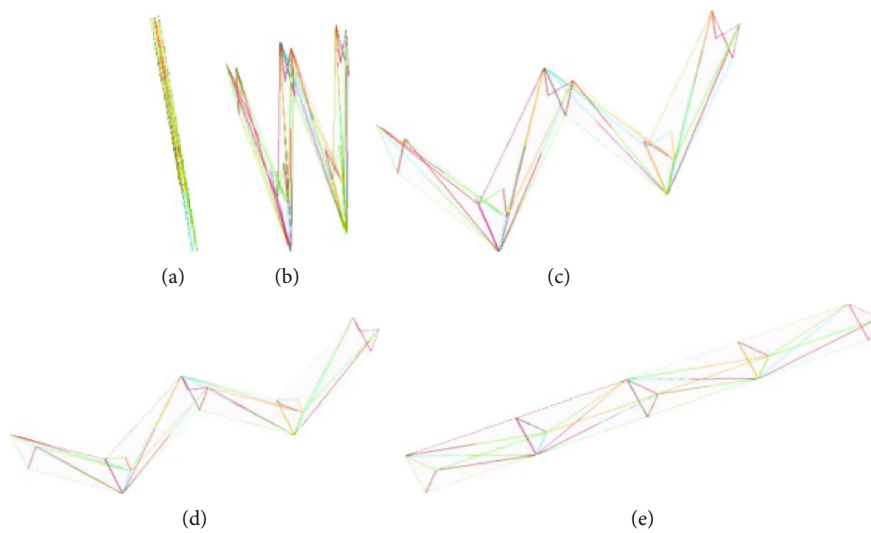FIGURE 7: Two-dimensional networking for triangular prism trusses based on cylindrical surface forming.

(a)   (b)   (c)

(d)   (e)

FIGURE 8: Motion simulation of the deployment of the 18R triangular prism truss mechanism.

(a) Stowed

(b) Deploying 1
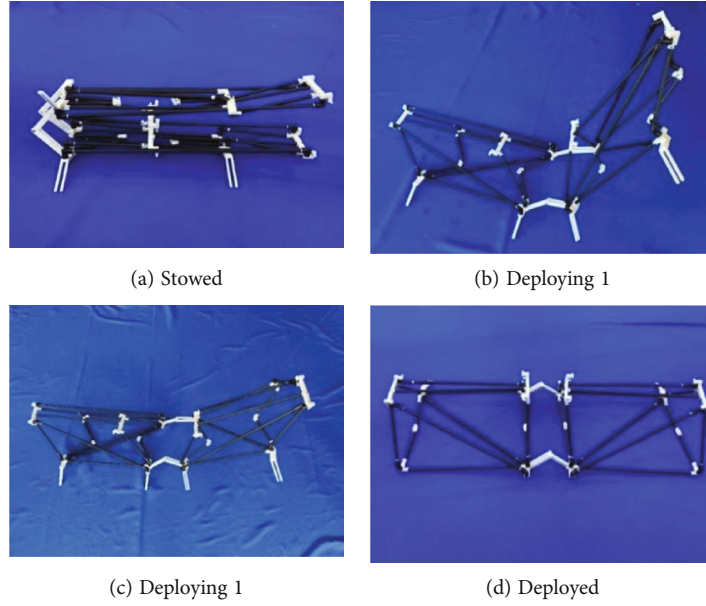
(c) Deploying 1

(d) Deployed

FIGURE 9: 2-unit longitudinal deployment principle prototype deployment test.
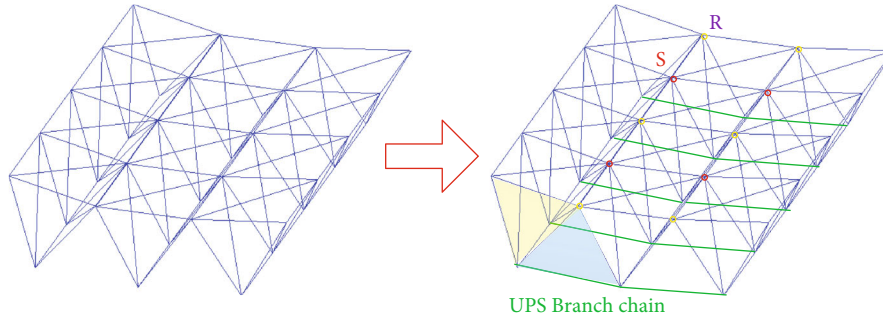

UPS Branch chain

FIGURE 10: Width-dimensional networking configuration of the 18R triangular prism truss mechanism.

According to Rule 2, we have the following constraints:

$$\begin{cases} e_S \leq v, \\ e_s \leq e_R + e_U. \end{cases} \quad (16)$$

Based on the above constraints, the combined mechanism can be obtained by configuring the kinematic pairs in the two-colour atlas for the mechanism.

Taking the two-colour topology diagram of the mechanism in Figure 4 as an example, $v = 12$, $v_t = 5$, and $e_G = 18$. If a single-degree-of-freedom mechanism ($\mu = 0$ and $M = 1$) without an overconstraint is constructed, then the parameters are brought into Equations (14), (15), and (16), and we obtain

$$\begin{cases} 5e_R + 4e_U + 3e_S = 70, \\ e_R + e_U + e_S = 18, \\ e_S \leq 12, \\ e_s \leq e_R + e_U. \end{cases} \quad (17)$$

Solving for the feasible configurations yields the following combinations:

$$\begin{cases} e_{R1} = 7, e_{U1} = 2, e_{S1} = 9, \\ e_{R2} = 6, e_{U2} = 4, e_{S2} = 8, \\ e_{R3} = 5, e_{U3} = 6, e_{S3} = 7, \\ e_{R4} = 4, e_{U4} = 8, e_{S4} = 6, \\ e_{R5} = 3, e_{U5} = 10, e_{S5} = 5, \\ e_{R6} = 2, e_{U6} = 12, e_{S6} = 4, \\ e_{R7} = 1, e_{U7} = 14, e_{S7} = 3, \\ e_{R8} = 0, e_{U8} = 16, e_{S8} = 2. \end{cases} \quad (18)$$

To simplify the mechanism, the first group of solutions with the most rotating pairs is taken, and a two-colour topology diagram that satisfies the rules is obtained, as shown in Figure 5.

The simulation verification suggests that the triangular prism unit deployment mechanism obtained by the graph
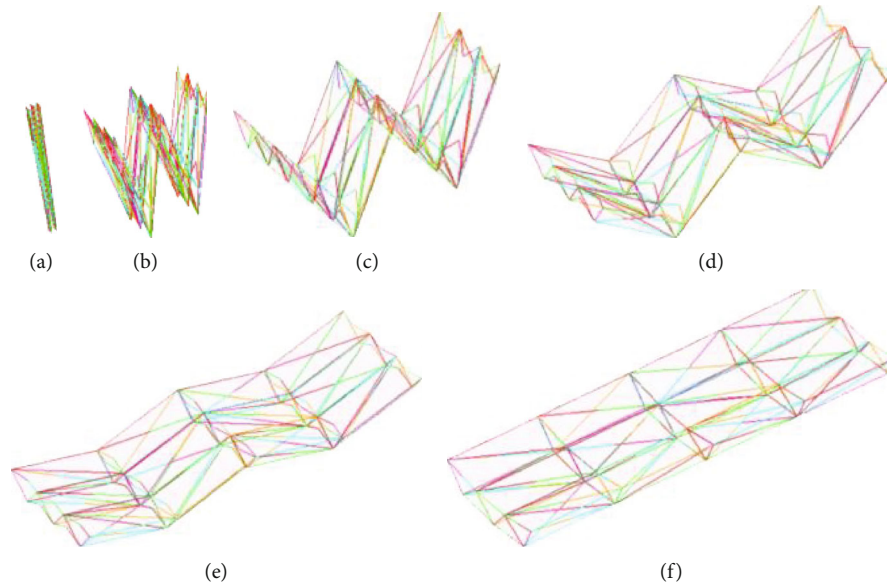
FIGURE 11: 18R triangular prism unit cylindrical network mechanism deployment motion simulation.

(a) Stowed
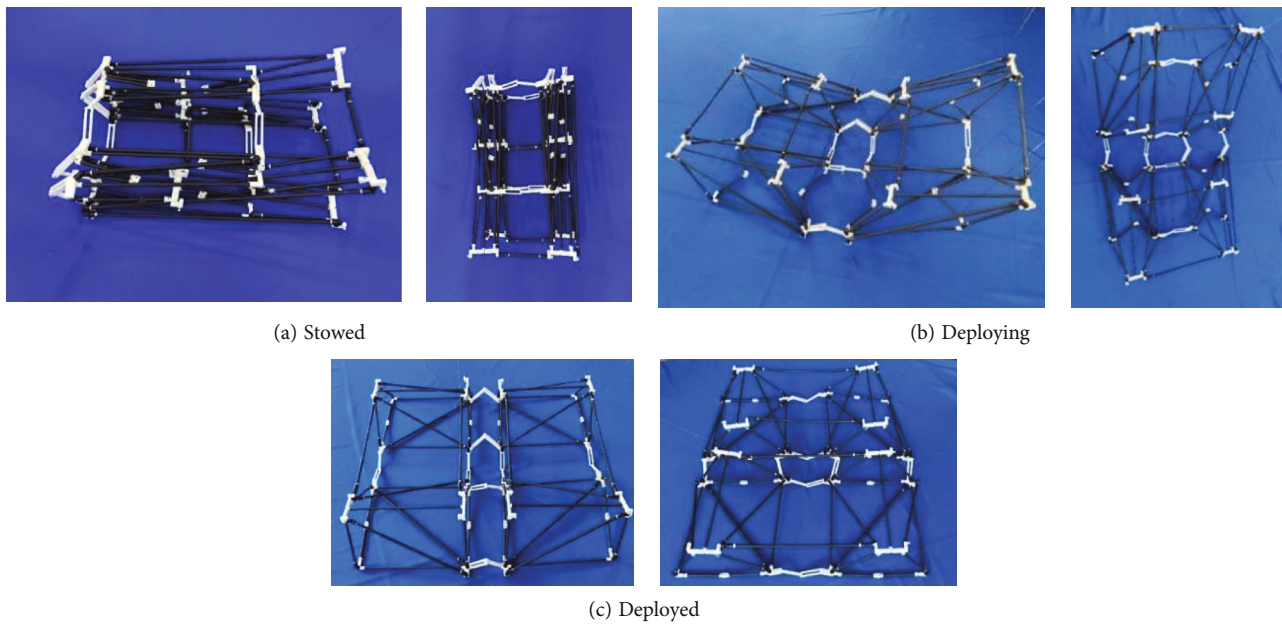
(b) Deploying

(c) Deployed

FIGURE 12: Four-unit horizontal and vertical deployment test.

theory configuration method can deploy with a single degree of freedom, and the triangular prism truss can be folded into a linear structure.

To achieve better local stiffness and deployment reliability in orbit, the on-board deployment mechanism often adopts an overconstrained mechanism. Based on the 7R2U9S triangular prism unit configuration, by changing all the U and S pairs into R pairs, an overconstrained 18R triangular prism unit mechanism can be obtained (Figure 6).

4. Triangular Prism Unit Mechanism Network Configuration

According to the structural characteristics of the parabolic cylindrical deployable antenna, the networking for triangular prism deployable elements can be divided into networking along the length and width directions, as shown in Figure 7. The modular structure of the whole parabolic cylindrical deployable antenna can be obtained by combining the networking in the two directions.
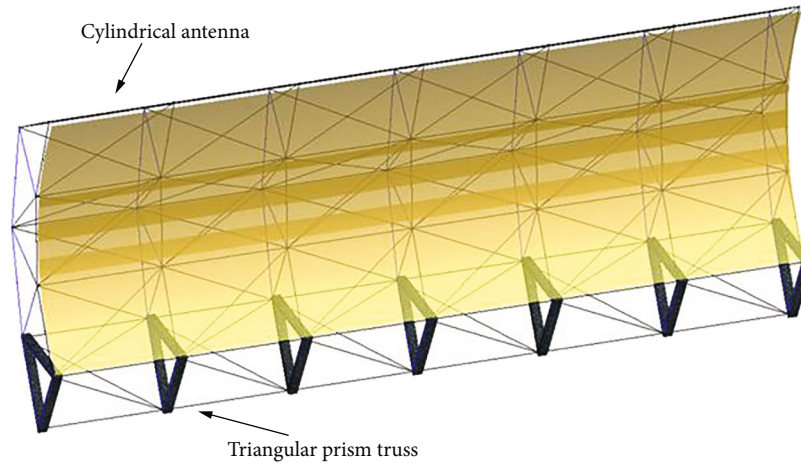
FIGURE 13: The process of antenna deployment.

4.1. Network along the Length Direction. The topology of the above single-degree-of-freedom triangular prism unit mechanism is carried out along the length direction, and the multiunit single-degree-of-freedom stowing and deployment are realized through the linkage structure. Through simulation verification, the single-degree-of-freedom stowing/deployment from the line to the space truss can be realized (Figure 8).

According to the joint configuration method proposed in this paper, the joints for the principle prototype are designed in detail, and a two-unit longitudinal expansion principle prototype is developed by 3D printing. The unfolding process is shown in Figure 9. The whole unfolding process is smooth and free of jamming, thereby proving the rationality and correctness of the configuration proposed in this paper.

4.2. Networking along the Width Direction. The stowed facet of the prismatic mechanism is used as the reflective surface. The S and R pairs are alternately arranged, and the back is closed by the UPS chain to release the rotational freedom between adjacent triangular prisms, the inconsistency in the apex angle of the triangle fitting curve is solved, and the triangular prism unit mechanism network structure is obtained (Figure 10).

Through simulation verification, the obtained triangular prism network structure can be used to realize the needed folding and deployment motions (Figure 11).

The deployment function of the four-unit principle prototypes in both the horizontal and vertical directions is tested. The deployment process is shown in Figure 12. The whole deployment process is smooth and free of jamming, which proves the rationality and correctness of the configuration.

5. Configuration Design of an Ultralarge Aperture Cylindrical Antenna

The general layout of the ultralarge aperture cylindrical antenna uses the triangular prism mechanism as the column
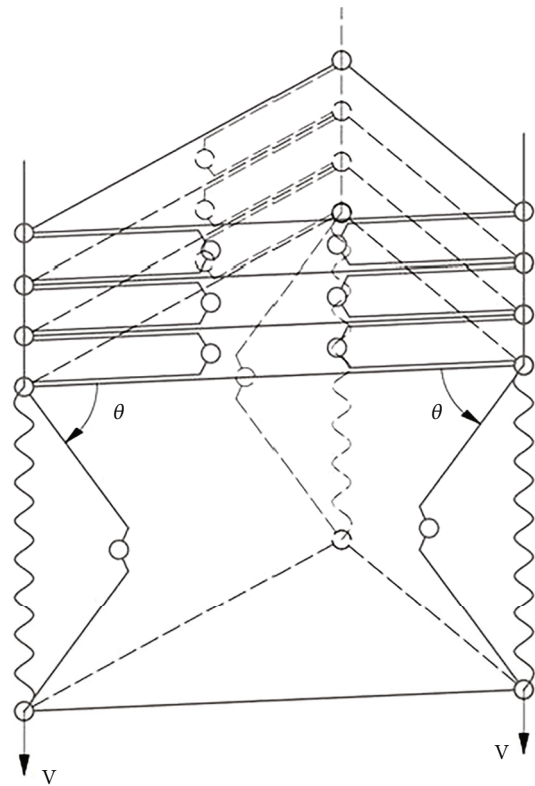

FIGURE 14: Triangular prism truss.

support structure, and a flat deployable phased array structure is used as the feed. The overall configuration of the mechanism is shown in Figure 13.

The triangular prism truss can be stowed into a plane [7]. This mechanism is based on the Sarrus mechanism, which is obtained by adding an RRR overconstrained branch chain (Figure 14).

The triangular prism deployable truss mechanism is composed of a lead screw synchronous drive component and triangular prism truss unit (Figure 15). According to the deployment length requirements, multiple deployable

(a) Stowed   (b) Deployed

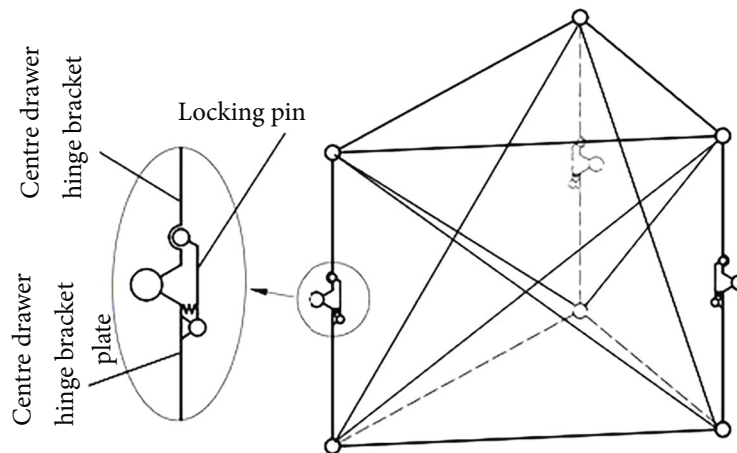FIGURE 15: Triprism deployable truss mechanism.

FIGURE 16: Triprism deployable unit.

truss units of the triangular prism are connected in series, the truss corners are connected with the three lead screws of the lead screw synchronous drive assembly, and the truss units are driven to deploy one by one through the lead screw drive.

In Figure 16, the deployment unit is composed of an upper triangular frame, a lower triangular frame, a folding bar, a locking hinge, a tension cable, and a screw nut. The upper and lower frames are triangles, which are mainly used to support the whole truss element and realize the

(a) Stowed   (b) Deployed
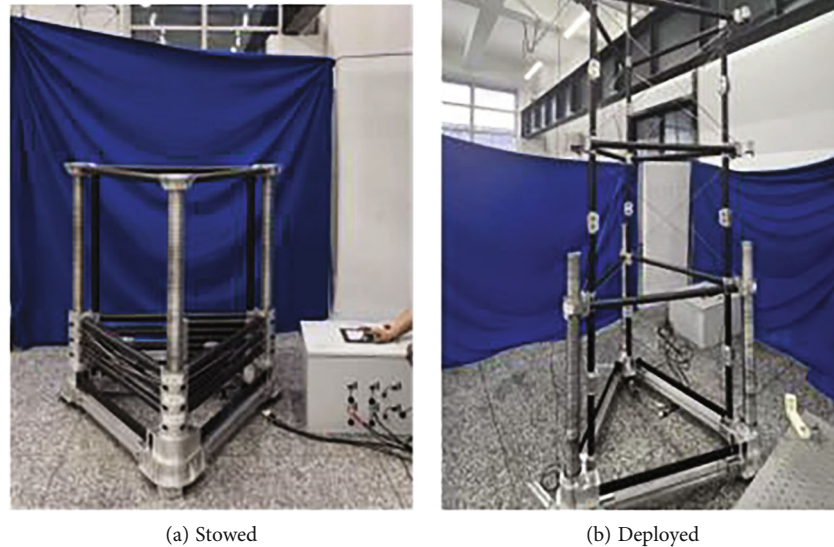
FIGURE 17: Development test of the engineering prototype.

synchronous drive and deployment of the lead screw. The folding bar is designed as two sections. The two sections of the folding bar are connected by locking hinges to realize the expansion and locking of the folding bar, which is constructed using a carbon fibre material. The tension cable produces a certain tension force on the deployed element, which effectively improves the stability and rigidity of the truss. The lead screw drives the upper triangular frame to complete the deployment movement.

As shown in Figure 17, a four-unit 10-metre-long deployable triangular prism truss prototype was developed. After the final assembly of the prototype, the deployment function test for the prototype is completed under the horizontal unloading state. Driven by the lead screw synchronization mechanism, the lead screw can rotate smoothly and synchronously, and the triangular prism truss can realize the function of gradual deployment. After deploying each unit in place, the folding bar is effectively locked with the expansion ability needed by the design.

Through prototype and deployment tests, the correctness of the configuration and design mechanism is verified.

6. Conclusion

The configuration synthesis for a triangular prism deployable mechanism is carried out by using graph theory. Various feasible deployable mechanisms are proposed using the method of graph theory. On the basis of a bicolour topology diagram, a mechanism topology diagram for a 12-bar mechanism is established, and the configuration for the motion pairs is completed. A single-degree-of-freedom 7R2U9S triangular prism unfolding element mechanism that can be folded into a linear stable truss is obtained. A method

for networking triangular prism unit mechanisms is proposed based on the geometric characteristics of parabolic cylindrical surfaces. Research into the configuration synthesis of unit network mechanisms based on graph theory provides a reference for the configuration synthesis of large deployable truss mechanisms.

Data Availability

The data used to support the findings of this study are included within the article.

Conflicts of Interest

The authors declare that there is no conflict of interest regarding the publication of this paper.

Acknowledgments

References

[1] C. Chen, J. Dong, J. Chen, F. Lin, S. Jiang, and T. Liu, "Research progress of large spaceborne parabolic antennas," *Journal of Aeronautics and Astronautics*, vol. 42, no. 1, pp. 1–21, 2021.

[2] X. Ma, Y. Li, Y. Xiao, S. Zheng, Z. Huang, and T. Feng, "Research status and prospect of large space deployable

antenna reflectors," *Space Electronics Technology*, vol. 2, pp. 16–26, 2018.

[3] I. Eastwood, D. Stephen, G. Sadowy, A. Huang, M. Lou, and B. Lopez, "System concept for the next-generation spaceborne precipitation radars," in *2000 IEEE Aerospace Conference. Proceedings (Cat. No.00TH8484)*, pp. 151–158, Big Sky, MT, USA, 2000.

[4] I. Eastwood and D. Stephen, "Next-generation spaceborne precipitation radar instrument concepts and technologies," in *45th AIAA Aerospace Sciences Meeting and Exhibit*, p. 1105, Reno, NV, USA, 2007.

[5] W. Alan and P. Sergio, "Tape-spring rolling hinges," in *Proceedings of 36th Aerospace Mechanisms Symposium, Glenn Research Center*, pp. 15–17, Cleveland, Sandusky, Ohio, 2002.

[6] O. Soykasap, A. Watt, and S. Pellegrino, "New deployable reflector concept," in *45th AIAA/ASME/ASCE/AHS/ASC Structures, Structural Dynamics & Materials Conference*, Palm Springs, CA, USA, 2004.

[7] L. Steven, W. Murphey, and M. Zatman, "Overview of the innovative space-based radar antenna technology program," *Journal of Spacecraft and Rockets*, vol. 48, no. 1, pp. 135–145, 2011.

[8] S. Lv, D. Zlatanov, and X. Ding, "Approximation of cylindrical surfaces with deployable Bennett networks," *Journal of Mechanisms and Robotics*, vol. 9, no. 2, pp. 1–6, 2017.

[9] H. Xiao, S. Lv, and X. Ding, "Design and analysis of a cable-driven deployable cylindrical mechanism," in *Proceedings of the ASME 2018 International Design Engineering*, pp. 1–8, Quebec, Canada, 2018.

[10] X. Song, Z. Deng, H. Guo, R. Liu, L. Li, and R. Liu, "Networking of Bennett linkages and its application on deployable parabolic cylindrical antenna," *Mechanism and Machine Theory*, vol. 109, pp. 95–125, 2017.

[11] NEC, "ANSARO-2, advanced satellite with new system architecture for observation-2," 2020, https://directory.eoportal.org/web/eoportal/satellite-missions/a/asnaro-2.

[12] B. Dong, H. Zhang, Y. Zhang, and N. Li, "Geometry modeling of truss structure for a space deployable parabolic cylindrical antenna," in *The 5th International Conference on Mechatronics and Mechanical Engineering (ICMME 2018)*, Wuhan, Hubei, China, 2019.

[13] F. Lin, C. Chen, J. Chen, and M. Chen, "Dimensional synthesis of antenna-deployable support structure," *International Journal of Aeronautical and Space Sciences*, vol. 21, no. 2, pp. 404–417, 2020.

[14] W. Herr and C. Horner, *Deployment Test of a 36-Element Tetrahedral Truss Module*, Vought Corp, Dallas, TX, USA, 1980.

[15] B. Warnaar and M. Chew, "Kinematic synthesis of deployable-foldable truss structures using graph theory, part 1: graph generation," *Journal of Mechanical Design*, vol. 117, no. 1, pp. 112–116, 1995.

[16] D. Tian, X. Fan, J. Zhang, L. Jin, R. Liu, and Y. Zhang, "Networking method for the structure of a large modular deployable space antenna," *International Journal of Aerospace Engineering*, vol. 2022, Article ID 4583374, 13 pages, 2022.

[17] A. Kazuhide, J. Mitsugi, and Y. Senbokuya, "Analyses of cable-membrane structure combined with deployable truss," *Computers & Structures*, vol. 74, no. 1, pp. 21–39, 2000.

[18] A. Meguro, K. Shintate, M. Usuib, and A. Tsujihata, "In-orbit deployment characteristics of large deployable antenna reflec-

[19] X. Chen and F. Guan, "A large deployable hexapod paraboloid antenna," *Journal of Astronautics*, vol. 22, no. 1, pp. 75–78, 2001.

[20] K. Vu, J. Liew, and K. Anandasivam, "Deployable tension-strut structures: from concept to implementation," *Journal of Constructional Steel Research*, vol. 62, no. 3, pp. 195–209, 2006.

[21] K. Vu, J. Liew, and K. Anandasivam, "Deployable tension-strut structures: structural morphology study and alternative form creations," *International Journal of Space Structures*, vol. 21, no. 3, pp. 149–164, 2006.

[22] J. Zhao, F. Chu, and Z. Feng, "The mechanism theory and application of deployable structures based on SLE," *Mechanism and Machine Theory*, vol. 44, no. 2, pp. 324–335, 2009.

[23] Y. Yang and X. Ding, "Kinematic analysis of a plane deployable mechanism assembled by four pyramid cells," *Acta Aeronautica Et Astronautica Sinica*, vol. 31, no. 6, pp. 1257–1265, 2010.

[24] Y. Yang and X. Ding, "Design and analysis of mast based on spatial polyhedral linkages mechanism along radial axes," *Journal of Mechanical Engineering*, vol. 47, no. 5, pp. 26–34, 2011.

[25] Y. Yang and W. Zhang, "Kinematic investigation and assembly application of a spatial symmetric 6R mechanism," *Acta Aeronautica et Astronautica Sinica*, vol. 35, no. 12, pp. 3459–3469, 2014.

[26] J. Cui, H. Huang, B. Li, and Z. Deng, "A novel surface deployable antenna structure based on special form of Bricard linkages," in *Second ASME/IFToMM International Conference on Reconfigurable Mechanisms and Robots*, pp. 783–792, Tianjin, China, 2012.

[27] X. Qi, Z. Deng, B. Li, R. Liu, and H. Guo, "Design and optimization of large deployable mechanism constructed by Myard linkages," *CEAS Space Journal*, vol. 5, no. 3-4, pp. 147–155, 2013.

[28] Y. Xu, L. Chen, W. Liu, J. Yao, J. Zhu, and Y. Zhao, "Type synthesis of the deployable mechanisms for the truss antenna using the method of adding constraint chains," *Journal of Mechanism and Robotics-Transactions of the AMSE*, vol. 10, no. 4, 2018.

[29] C. Shi, H. Guo, M. Li, R. Liu, and Z. Deng, "Conceptual configuration synthesis of line-foldable type quadrangular prismatic deployable unit based on graph theory," *Mechanism & Machine Theory*, vol. 121, pp. 563–582, 2018.

[30] C. Shi, H. Guo, Z. Zheng, M. Li, R. Liu, and Z. Deng, "Conceptual configuration synthesis and topology structure analysis of double-layer hoop deployable antenna unit," *Mechanism & Machine Theory*, vol. 129, pp. 232–260, 2018.

[31] B. Han, Y. Xu, Y. Han, J. Yao, and Y. Zhao, "Type synthesis of ring truss deployable antenna mechanism based on screw theory," *Journal of Astronautics*, vol. 40, no. 7, pp. 831–841, 2019.

[32] Z. Deng, *Design of Space Deployable and Foldable Mechanisms*, Harbin Institute of Technology Press, Harbin, China, 2013.

[33] Y. Wang, Z. Deng, R. Liu, and H. Guo, "An efficient algorithm for detecting isomorphism of deployable truss structures using incident degree," in *International Conference on Electronic and Mechanical Engineering and Information Technology*, pp. 345-346, Harbin, China, 2011.